

Article

Sesquiterpenoids from the Florets of *Carthamus tinctorius* (Safflower) and Their Anti-Atherosclerotic Activity

Lei Li ^{1,2,3,†}, Juan Liu ^{1,2,3,†}, Xinrui Li ^{1,2,3}, Yuqin Guo ^{1,2,3}, Yunqiu Fan ^{1,2,3}, Hongzhen Shu ^{1,2,3}, Guangxu Wu ^{1,2,3}, Cheng Peng ^{1,2,*} and Liang Xiong ^{1,2,3,*} 

¹ State Key Laboratory of Southwestern Chinese Medicine Resources, Chengdu University of Traditional Chinese Medicine, Chengdu 611137, China

² School of Pharmacy, Chengdu University of Traditional Chinese Medicine, Chengdu 611137, China

³ Institute of Innovative Medicine Ingredients of Southwest Specialty Medicinal Materials, Chengdu University of Traditional Chinese Medicine, Chengdu 611137, China

* Correspondence: pengcheng@cducm.edu.cn (C.P.); xiling0505@126.com (L.X.)

† These authors contributed equally to this work.

Abstract: (1) Background: The florets of *Carthamus tinctorius* L. are traditionally used as a blood-activating drug and can be used for the treatment of atherosclerosis, but no compounds with anti-atherosclerotic activity have been reported. (2) Methods: This study investigated the chemical compounds from the florets of *C. tinctorius*. Comprehensive spectroscopic techniques revealed their structures, and ECD calculations established their absolute configurations. Nile Red staining, Oil Red O staining, and cholesterol assessment were performed on these compounds and their aglycones for the inhibitory activity against the formation of foam cells induced by oxidized low-density lipoprotein (ox-LDL) in RAW264.7 macrophages. In addition, RAW264.7 macrophages were tested for their anti-inflammatory activity by measuring the inhibition of NO production caused by LPS. (3) Results: Five new sesquiterpenoids (1–5) isolated from the florets of *C. tinctorius* were identified as (–)-(1*R*,4*S*,9*S*,11*R*)-caryophyll-8(13)-en-14-ol-5-one (1), (+)-(1*R*,4*R*,9*S*,11*R*)-caryophyll-8(13)-en-14-ol-5-one (2), (–)-(3*Z*,1*R*,5*S*,8*S*,9*S*,11*R*)-5,8-epoxycaryophyll-3-en-14-*O*-β-D-glucopyranoside (3), (+)-(1*S*,7*R*,10*S*)-guai-4-en-3-one-11-*O*-β-D-fucopyranoside (4), and (–)-(2*R*,5*R*,10*R*)-vetispir-6-en-8-one-11-*O*-β-D-fucopyranoside (5). All compounds except for compound 3 reduced the lipid content in ox-LDL-treated RAW264.7 cells. Compounds 3 and 4 and their aglycones were found to reduce the level of total cholesterol (TC) and free cholesterol (FC) in ox-LDL-treated RAW264.7 cells. However, no compounds showed anti-inflammatory activity. (4) Conclusion: Sesquiterpenoids from *C. tinctorius* help to decrease the content of lipids, TC and FC in RAW264.7 cells, but they cannot inhibit NO production, which implies that their anti-atherogenic effects do not involve the inhibition of inflammation.

Keywords: *Carthamus tinctorius*; sesquiterpenoids; structure elucidation; RAW264.7 cells; anti-atherogenic activity



Citation: Li, L.; Liu, J.; Li, X.; Guo, Y.; Fan, Y.; Shu, H.; Wu, G.; Peng, C.; Xiong, L. Sesquiterpenoids from the Florets of *Carthamus tinctorius* (Safflower) and Their Anti-Atherosclerotic Activity. *Nutrients* **2022**, *14*, 5348. <https://doi.org/10.3390/nu14245348>

Academic Editor: Francesca Giampieri

Received: 28 October 2022

Accepted: 10 December 2022

Published: 16 December 2022

Publisher's Note: MDPI stays neutral with regard to jurisdictional claims in published maps and institutional affiliations.



Copyright: © 2022 by the authors. Licensee MDPI, Basel, Switzerland. This article is an open access article distributed under the terms and conditions of the Creative Commons Attribution (CC BY) license (<https://creativecommons.org/licenses/by/4.0/>).

1. Introduction

Cardiovascular diseases have recently topped the list of causes of diseases in general, posing an immediate danger to human health. Atherosclerosis (AS) is a major pathological basis for many cardiovascular and cerebrovascular diseases, and macrophages play a major role in the plaque formation process of AS. In the early stages of AS development, macrophages phagocytose oxidize more low-density lipoprotein (ox-LDL) than they can metabolize, causing their massive accumulation of lipids and turning into foam cells. Then, foam cells gather together under the vascular endothelium to form a raised plaque, which further narrows or blocks blood vessels, thereby promoting the development of AS [1,2]. Therefore, inhibition of macrophage foaminess can effectively treat AS.

cross-peaks from H₂-14 to C-1, C-10, C-11, and C-15. An NOESY experiment was applied to identify the relative configuration of compound **1**. Correlations of H-9/H₃-15 and H-1/H-4 and H₂-14 (Figure 3) suggested that H-9 and Me-11 were co-facial, whereas H-1, H-4, and hydroxymethyl-11 occupied the opposite face. By comparing the computed electronic circular dichroism (ECD) data of compound **1** with the experimental ECD data (Figure 4), the absolute configuration of compound **1** was revealed to be 1*R*,4*S*,9*S*,11*R*. Therefore, compound **1** was determined to be (–)-(1*R*,4*S*,9*S*,11*R*)-caryophyll-8(13)-en-14-ol-5-one.

Table 1. ¹H NMR data of compounds **1–3** and **3a** in CD₃OD (δ in ppm, *J* in Hz).

No.	1	2	3	3a
1	1.83 m	1.64 m	2.17 m	2.07–2.01 m
2	1.43 m	1.65 m	2.07 m	2.07–2.01 m
	1.38 m	1.32 m		
3	1.75 m	1.81 m	5.38 m	5.38 m
	1.55 m	1.64 m		
4	2.67 m	2.60 m		
5			4.50 dd (9.6, 5.4)	4.51 dd (9.6, 5.4)
	2.64 m	2.62 m	2.49 m	2.49 m
6	2.39 m	2.50 m	2.01 m	2.07–2.01 m
	2.48 m	2.48 m	2.37 m	2.30 m
7	2.37 m		1.61 m	1.61 m
	2.23 m	2.46 m	2.11 m	2.07–2.01 m
9				
10	1.79 dd (10.8, 10.2)	1.73 dd (10.8, 10.2)	1.69 dd (10.8, 10.2)	1.52 dd (10.2, 10.2)
	1.54 dd (10.8, 9.0)	1.47 dd (10.2, 8.4)	1.45 dd (10.2, 7.8)	1.42 dd (10.2, 7.8)
12	1.03 d (7.2)	1.01 d (6.6)	1.66 s	1.65 s
13	5.05 brs	4.93 brs	1.18 s	1.18 s
	5.01 brs	4.90 brs		
14	3.24 d (11.4)	3.20 d (11.4)	3.68 d (10.2)	3.25 d (10.8)
			3.24 d (10.2)	
15	0.97 s	0.99 s	1.07 s	1.03 s
1'			4.24 d (7.8)	
2'			3.19 dd (9.0, 7.8)	
3'			3.33 t (9.0)	
4'			3.27 t (9.0)	
5'			3.27 ddd (9.0, 6.0, 2.4)	
6'			3.86 dd (12.0, 2.4)	
			3.67 dd (12.0, 6.0)	

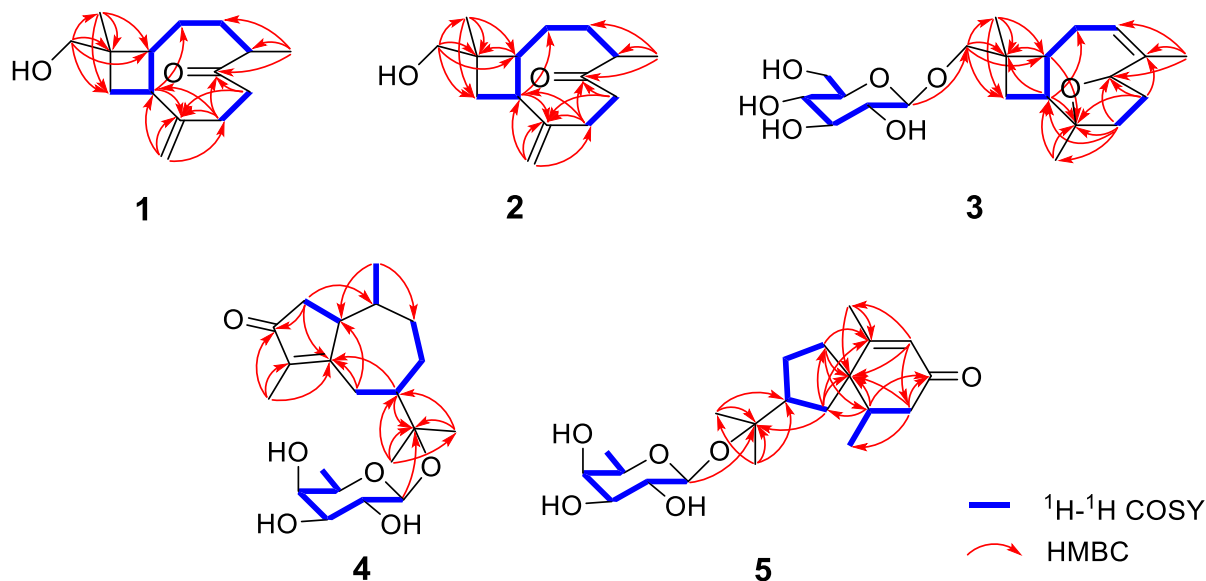


Figure 2. Key ¹H–¹H COSY and HMBC correlations of compounds **1–5**.

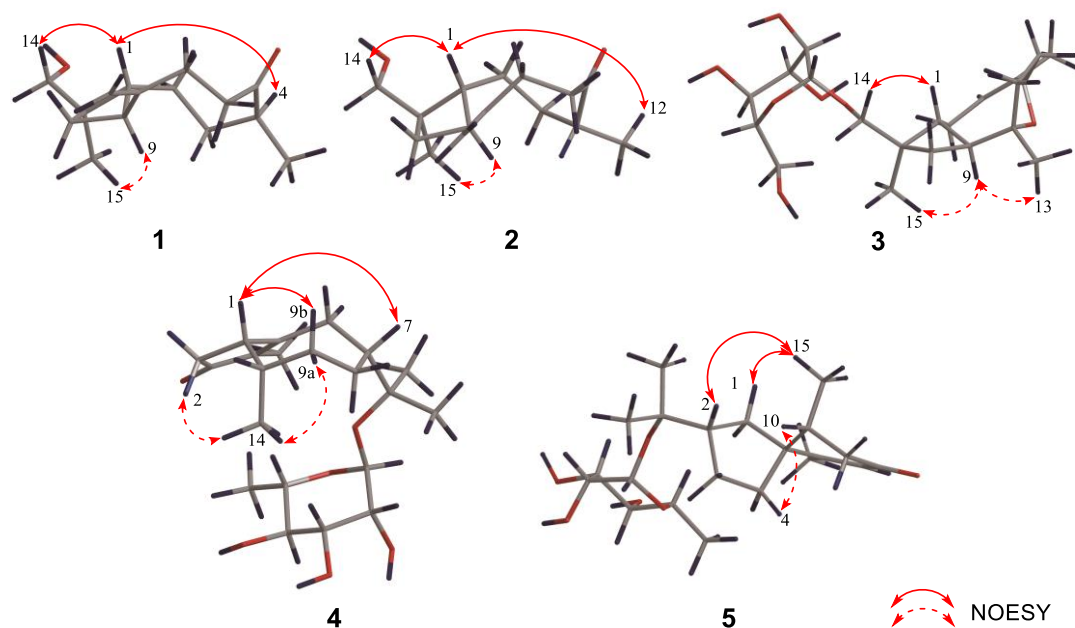


Figure 3. Key NOESY correlations of compounds 1–5.

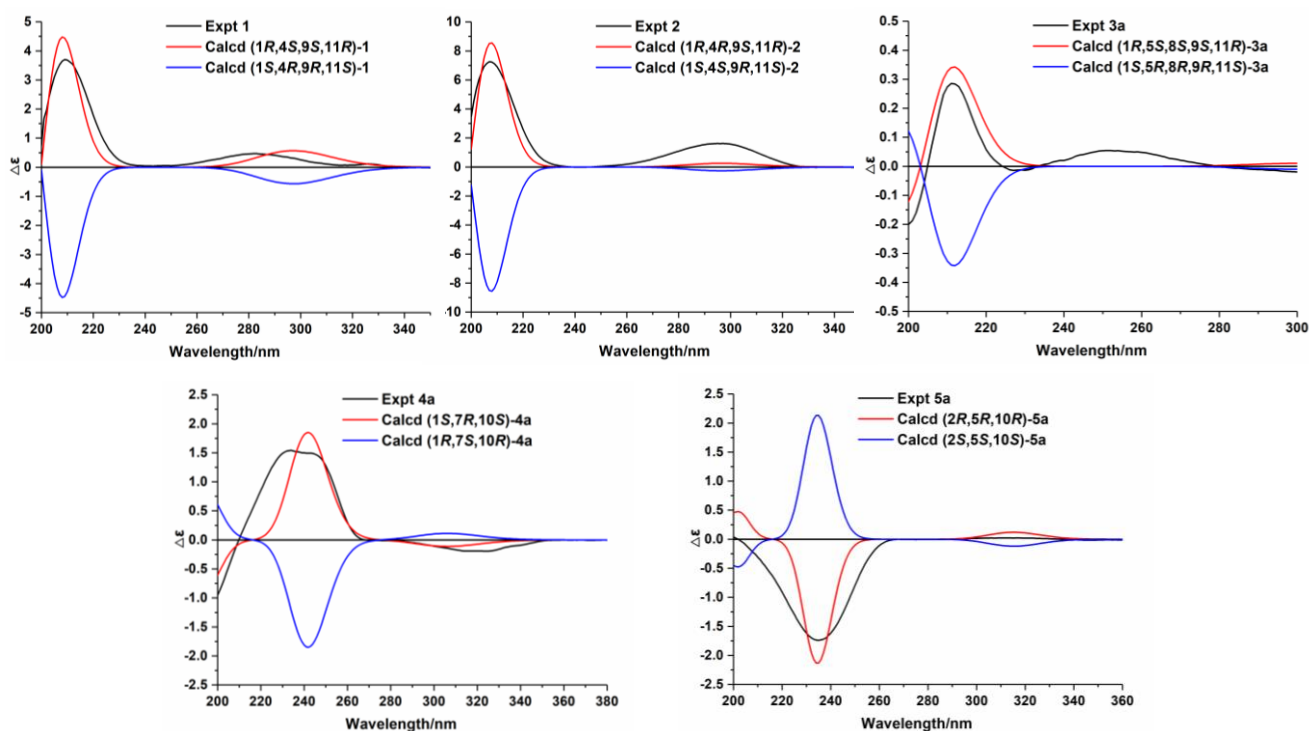


Figure 4. Experimental and calculated ECD spectra of compounds 1–2 and 3a–5a. Based on the HR-ESI-MS data of compound 2, its chemical formula is similar to that of compound 1. The ^1H , ^{13}C , and 2D NMR spectra of compounds 2 and 1 showed that the planar structures of these two compounds are identical. Further analysis revealed that compound 2 was a C-4 epimer of compound 1 based on the NOESY correlations of $\text{H}_2\text{-14}/\text{H-1}$, $\text{H-1}/\text{H}_3\text{-12}$, and $\text{H-9}/\text{H}_3\text{-15}$ (Figure 3). Moreover, ECD calculations showed that the absolute configuration of compound 2 is $1R,4R,9S,11R$ (Figure 4). Therefore, compound 2 was identified as (+)-(1*R*,4*R*,9*S*,11*R*)-caryophyll-8(13)-en-14-ol-5-one.

Table 2. ^{13}C NMR data of compounds 1–5 in CD_3OD (δ in ppm).

No.	1	2	3	4	5
1	49.6	47.7	41.0	47.2	32.5
2	27.2	28.8	30.9	42.3	52.2
3	31.2	32.3	124.1	211.3	28.8
4	48.6	49.0	140.8	138.3	35.9
5	219.4	220.0	82.0	181.1	51.7
6	42.9	43.4	35.5	35.3	173.3
7	35.7	33.0	32.2	47.3	125.9
8	155.1	154.0	87.3	28.5	202.4
9	44.1	44.5	50.4	38.0	43.6
10	35.6	34.3	31.7	36.8	38.5
11	39.3	39.8	39.0	81.3	79.2
12	17.2	17.2	26.3	22.8	26.2
13	112.4	112.1	26.7	25.2	24.7
14	71.0	71.2	78.1	12.5	21.3
15	17.6	17.6	17.0	7.9	16.8
1'			104.7	98.9	98.9
2'			75.8	72.5	72.6
3'			78.4	75.3	75.4
4'			71.7	73.1	73.1
5'			77.9	71.4	71.5
6'			62.8	16.8	17.1

Compound **3** has a molecular formula of $\text{C}_{21}\text{H}_{34}\text{O}_7$, as determined by the HR-ESI-MS. The ^1H , ^{13}C , and DEPT NMR data of compound **3** suggested that it is also a caryophyllane-type sesquiterpenoid. The signals for an anomeric proton [δ_{H} 4.24 (d, $J = 7.8$ Hz)] and an anomeric carbon (δ_{C} 104.7) revealed the existence of a β -glucosyl [25], indicating that compound **3** is a caryophyllane glycoside. In addition, the ^1H and ^{13}C NMR data (Tables 1 and 2) exhibited signals attributed to an olefinic methine [δ_{H} 5.38 (1H, m, H-3), δ_{C} 124.1], an oxygenated methine [δ_{H} 4.50 (1H, dd, $J = 9.6, 5.4$ Hz, H-5), δ_{C} 82.0], an oxygenated quaternary carbon (δ_{C} 87.3), and an olefinic quaternary carbon (δ_{C} 140.8) in the aglycone unit. Thus, the existence of an epoxy moiety and a trisubstituted double bond was deduced based on the molecular formula. Comparison of the NMR data between compound **3** and $5\alpha,8\alpha$ -epoxycaryophyll-3-ene [26] suggested that an additional β -glucose moiety and an oxygenated methene group in compound **3** replaced a methyl group (C-14) in $5\alpha,8\alpha$ -epoxycaryophyll-3-ene, and this deduction was confirmed by the HMBC correlation from H-1' to C-14.

In the NOESY spectrum of compound **3**, cross-peaks of H₂-14/H-1 and H-9/H₃-15 demonstrated the same orientation of H₂-14 and H-1, whereas H-9 and H₃-15 had the opposite orientation. The orientation of the 5-O-8 bridge was established by an NOE signal of H-9/H₃-13. In addition, an NOE interaction between H-3 and H₃-12 disclosed a Z-geometry for Δ^3 . To verify the absolute configuration of compound **3**, it was subjected to enzymatic hydrolysis, which yielded an aglycone **3a** and a D-glucose. Then, ECD calculation was carried out to resolve the absolute configuration of **3a**. As depicted in Figure 4, the calculated ECD spectrum of (1*R*,5*S*,8*S*,9*S*,11*R*)-**3a** and the experimental ECD spectrum of **3a** were in good agreement. Therefore, it was concluded that compound **3** is (–)-(3*Z*,1*R*,5*S*,8*S*,9*S*,11*R*)-5,8-epoxycaryophyll-3-en-14-*O*- β -D-glucopyranoside.

The molecular formula of compound **4** was identified as $\text{C}_{21}\text{H}_{34}\text{O}_6$ by HR-ESI-MS at m/z 405.2244 [$\text{M}+\text{Na}$]⁺ (calcd for 405.2253). The ^1H NMR spectrum (Table 3) exhibited distinguishable signals of five oxygenated methines [δ_{H} 4.42 (1H, d, $J = 7.8$ Hz, H-1'), 3.58 (1H, q, $J = 6.6$ Hz, H-5'), 3.56 (1H, d, $J = 3.6$ Hz, H-4'), 3.46 (1H, dd, $J = 9.6, 3.6$ Hz, H-3'), and 3.42 (1H, dd, $J = 9.6, 7.8$ Hz, H-2')], which might be attributable to a β -glycosyl moiety. Additionally, five methyl groups [δ_{H} 0.64 (3H, d, $J = 7.2$ Hz, H₃-14), 1.09 (3H, d, $J = 6.6$ Hz, H₃-6'), 1.21 (3H, s, H₃-12), 1.33 (3H, s, H₃-13), and 1.66 (3H, s, H₃-15)] were deducible from the ^1H NMR data. The ^{13}C NMR (Table 2) and the DEPT data revealed 21 carbon resonances

attributed to the above units, four aliphatic methylenes, three aliphatic methines, and four quaternary carbons [an α,β -unsaturated ketone unit (δ_C 211.3, 138.3, and 181.1) and an oxygenated quaternary carbon (δ_C 81.3)]. Comprehensive analysis of the ^1H - ^1H COSY, HSQC, and HMBC spectra indicated that the planar structure of compound **4** is similar to (1*R*,7*R*,10*S*)-11-*O*- β -D-glucopyranosyl-4-guaien-3-one [27], except for the glycosyl unit C-11. The glycosyl unit in compound **4** was further determined to be β -D-fucosyl due to the coupling constants ($J_{1',2'} = 7.8$ Hz, $J_{2',3'} = 9.6$ Hz, $J_{3',4'} = 3.6$ Hz, and $J_{4',5'} \approx 0$ Hz), together with the ^{13}C NMR data (δ_C 98.9, 72.5, 75.3, 73.1, 71.4, and 16.8) [20,28]. The NOESY correlations of H-1/H-7, H-1/H-9b, H₃-14/H-9a, and H₃-14/H-2b (Figure 3) were used to ascertain the relative structure of the aglycone moiety in compound **4**. Enzymatic hydrolysis of compound **4** provided the aglycone **4a**. Comparison of the experimental and calculated ECD spectra of **4a** (Figure 4) assigned 1*S*,7*R*,10*S* configuration to **4a**. Consequently, compound **4** was determined to be (+)-(1*S*,7*R*,10*S*)-guai-4-en-3-one-11-*O*- β -D-fucopyranoside.

Table 3. ^1H NMR data of compounds **4**, **4a**, **5**, and **5a** in CD₃OD (δ in ppm, J in Hz).

No.	4	4a	5	5a
1	3.20 m	3.22 m	1.98 dd (13.8, 7.2) 1.67 dd (13.8, 12.0)	1.92 dd (13.8, 7.2) 1.55 dd (13.8, 12.0)
2	2.55 dd (18.6, 6.0) 2.03 d (18.6)	2.58 dd (18.6, 6.0) 2.03 d (18.6)	2.17 m	2.07 m
3			1.84 m	1.86 m
4			1.84 m	1.86 m
6	3.38 m 2.18 m	3.38 m 2.27 m		
7	1.95 m	2.04 m	5.74 brs	5.75 brs
8	1.92 m 1.30 m	1.95 m 1.30 m		
9	1.85 m 1.77 m	1.87 m 1.75 m	2.42 dd (16.8, 4.2) 2.24 dd (16.8, 9.6)	2.45 dd (16.8, 4.2) 2.24 dd (16.8, 9.6)
10	2.13 m	2.14 m	2.10 m	2.12 m
12	1.21 s	1.19 s	1.27 s	1.21 s
13	1.33 s	1.24 s	1.26 s	1.21 s
14	0.64 d (7.2)	0.64 d (7.2)	2.04 d (1.2)	2.02 d (0.6)
15	1.66 s	1.66 s	1.05 d (6.6)	1.04 d (6.6)
1'	4.42 d (7.8)		4.42 d (7.8)	
2'	3.42 dd (9.6, 7.8)		3.41 dd (9.6, 7.8)	
3'	3.46 dd (9.6, 3.6)		3.47 dd (9.6, 3.6)	
4'	3.56 d (3.6)		3.59 d (3.6)	
5'	3.58 q (6.6)		3.62 q (6.0)	
6'	1.09 d (6.6)		1.24 d (6.0)	

The HR-ESI-MS of compound **5** revealed that it is a structural isomer of compound **4**. Comparative analysis of their ^1H and ^{13}C NMR data exhibited that they share similar functional groups such as an α,β -unsaturated ketone unit, four methyl groups, and a β -D-fucosyl moiety. However, as shown in Figure 2, 2D NMR data analysis pointed out that compound **5** is a vetispirane-type sesquiterpenoid [29]. The NOESY correlations of H₃-15/H-1a, H-10/H₂-4, and H-2/H₃-15 (Figure 3) determined the relative structure of compound **5**. Similar to compound **4**, the aglycone **5a** was produced by enzymatic hydrolysis of compound **5**, and 2*R*,5*R*,10*R* configuration was assigned to **5a** according to ECD calculations (Figure 4). Therefore, the structure of compound **5** was established as (−)-(2*R*,5*R*,10*R*)-vetispir-6-en-8-one-11-*O*- β -D-fucopyranoside.

2.2. Anti-Atherosclerotic Activity of Compounds 1–5 and Aglycones 3a–5a

The anti-atherosclerotic activity of the isolates (1–5) and their aglycones (3a–5a) was evaluated by detecting their inhibitory effects against RAW264.7 cell foaming induced by ox-LDL (Yiyuan Biotechnologies, Guangzhou, China) [1,30]. First, a CCK-8 assay was applied to evaluate the effects of the eight compounds on RAW264.7 cell viability, and all of the compounds were found to be noncytotoxic. Then, they were tested for anti-macrophage foaming activity by reducing the content of lipid in RAW264.7 cells treated by ox-LDL. As depicted in Figure 5, all compounds, except for compound 3, showed significant activity by Nile Red staining. In particular, the effects of compounds 1, 2, 3a, 4a, 5, and 5a were equal to or superior to the effect of the positive control (25 μ M of simvastatin). Interestingly, all of the aglycones (3a–5a) had better effects than their glycosides (3–5), which suggests that glycosidation of the sesquiterpenoids of safflower may result in a decrease in their anti-atherosclerotic activity. Although compound 4 showed weak activity in Nile Red staining, a significant effect was observed for compound 4 in Oil Red O staining (Figure 6). Specifically, compared with the control group, the model group collected more Oil Red O-stained lipid. In the drug group, compound 4 significantly decreased Oil Red O-stained lipid accretion.

To further explore the anti-atherosclerotic activity of compounds 3, 3a, 4, and 4a, the total cholesterol (TC) and free cholesterol (FC) levels in foamy macrophages were assessed by ELISA (Shanghai Keshun Science and Technology Co., Ltd., Shanghai, China). As shown in Figure 7, compounds 3, 3a, 4, and 4a significantly decreased the levels of TC and FC in ox-LDL-treated RAW264.7 cells in a dose-dependent way ($p < 0.01$ vs. model group). In addition, all compounds were investigated for their ability to inhibit lipopolysaccharide-induced NO production in RAW264.7 cells. The results showed that none of the compounds had an anti-inflammatory effect. Thus, it can be inferred that the safflower sesquiterpenoids do not exert their anti-atherogenic effects through the anti-inflammatory pathway [31]. Unfortunately, no further investigations on the molecular mechanisms were carried out due to the limited sample quantities of the isolates.

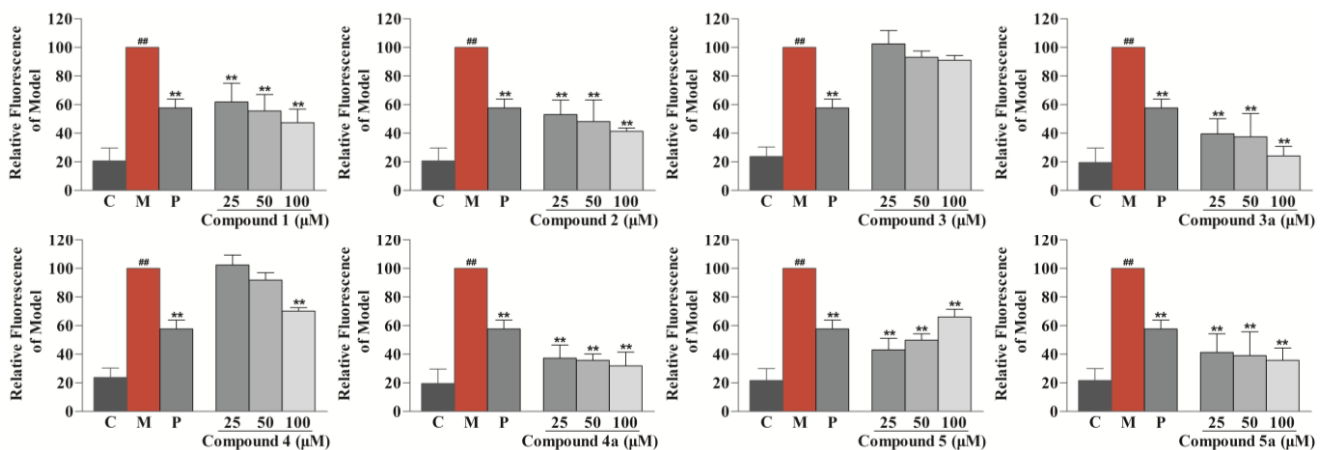


Figure 5. Effects of compounds 1–5 and 3a–5a to inhibit lipid drops accumulation in ox-LDL-treated RAW264.7 cells determined by Nile Red staining. Results are expressed as the mean \pm SD ($n = 3$). Model group was subject to 75 μ g/mL ox-LDL. Positive group was subject to 25 μ M simvastatin. ## $p < 0.01$ vs. control group; ** $p < 0.01$ vs. model group. C: control group, M: model group, and P: positive group.

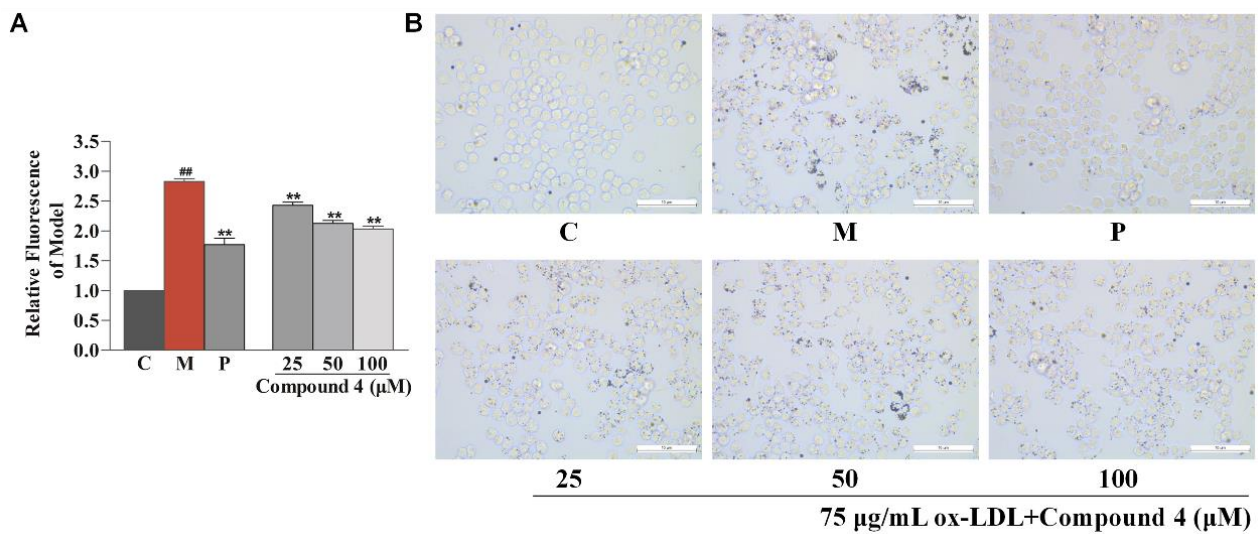


Figure 6. Inhibitory effects of compound 4 against lipid drops accumulation in ox-LDL-treated RAW264.7 cells measured by Oil Red O staining. (A) Oil Red O content evaluated by isopropanol extraction. (B) Oil Red O staining images of RAW264.7 cells (magnification 400×). Results are expressed as the mean ± SD ($n = 3$). Model group was subject to 75 μg/mL ox-LDL. Positive group was subject to 25 μM simvastatin. ^{##} $p < 0.01$ vs. control group; ^{**} $p < 0.01$ vs. model group.

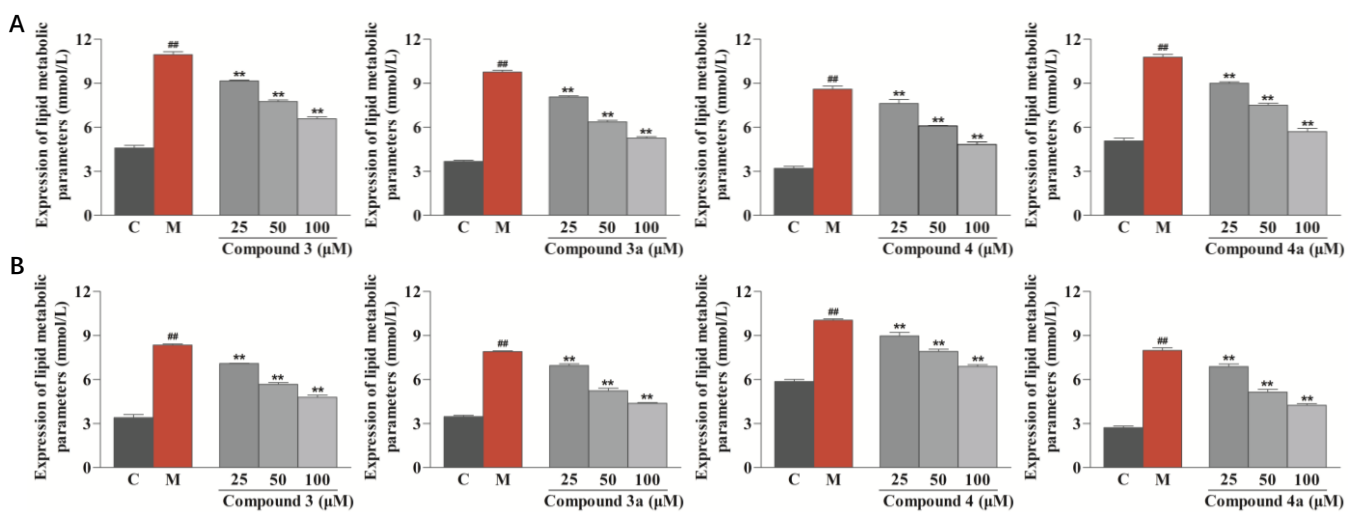


Figure 7. Effects of compounds 3, 3a, 4, and 4a on the contents of TC and FC in ox-LDL-treated RAW264.7 cells evaluated by ELISA. (A) Effects of compounds 3, 3a, 4, and 4a on the intracellular content of TC. (B) Effects of compounds 3, 3a, 4, and 4a on the intracellular content of FC. Results are expressed as the mean ± SD ($n = 3$). Model group was subject to 75 μg/mL ox-LDL. ^{##} $p < 0.01$ vs. control group; ^{**} $p < 0.01$ vs. model group.

3. Experimental Section

3.1. General Experimental Procedures

General experimental instruments and materials are shown in Text S1, Supplementary Materials.

3.2. Plant Material

The florets of *C. tinctorius* were gathered from Luole Village, Sichuan Province, China. The sample was authenticated by Dr. Ji-hai Gao (Chengdu University of TCM, Chengdu, China). A voucher specimen (No. CT-20180608) was placed at the State Key Laboratory of Southwestern Chinese Medicine Resources, Chengdu University of TCM.

3.3. Extraction and Isolation

The florets of *C. tinctorius* (50 kg) were decocted twice with 12 times the quantity of H₂O for 1 h each time. The extract was concentrated under reduced pressure in a big rotary evaporator (10 L) at 55 °C to produce a residue (16 kg). The residue was separated on a D-101 macroporous adsorbent resin (Sinopharm Chemical Reagent Co., Ltd., Shanghai, China) column using a gradient of H₂O, 20%, 50%, 70%, and 90% EtOH to afford five fractions (A–E). Fraction D (66.7 g) was performed on a silica gel column (Yantai Institute of Chemical Technology, Yantai, China) and eluted with a gradient of CH₂Cl₂/MeOH (1:0–0:1) to afford 14 major fractions (D₁–D₁₄). D₇ (6 g) was chromatographed on RP-MPLC eluted with MeOH/H₂O (20:80–100:0) to obtain 10 subfractions (D₇₋₁–D₇₋₁₀). Six sub-subfractions (D₇₋₃₋₁–D₇₋₃₋₆) were obtained from D₇₋₃ by silica gel column chromatography with a gradient elution system of CH₂Cl₂/MeOH (50:1–1:1). D₇₋₃₋₁ was further separated into D₇₋₃₋₁₋₁–D₇₋₃₋₁₋₇ by column chromatography over Toyopearl HW-40F (Tosoh Corp., Tokyo, Japan) using 50% MeOH as the eluent. Compound 4 (3.5 mg) was derived from D₇₋₃₋₁₋₂ by RP semipreparative HPLC (75% MeOH in H₂O). D₇₋₃₋₁₋₃ was further separated by TLC (CH₂Cl₂/MeOH, 10:1), followed by RP semipreparative HPLC (75% MeOH in H₂O), to obtain compound 5 (2 mg). Separation of D₇₋₃₋₁₋₄ by semipreparative HPLC (MeOH/H₂O, 75:25) yielded compounds 1 (0.8 mg) and 2 (0.7 mg). D₇₋₃₋₂ was separated by silica gel column chromatography and eluted with a gradient elution of CH₂Cl₂/MeOH (200:1–1:1) to yield D₇₋₃₋₂₋₁–D₇₋₃₋₂₋₆. From D₇₋₃₋₂₋₅, compound 3 (3.0 mg) was obtained by TLC using CH₂Cl₂–MeOH (10:1) as the developing solvent.

3.4. Spectroscopic Data

(–)-(1*R*,4*S*,9*S*,11*R*)-Caryophyll-8(13)-en-14-ol-5-one (1): colorless oil; $[\alpha]_{\text{D}}^{20}$ – 4.2 (*c* 0.02, MeOH); IR ν_{max} 3437, 2957, 2925, 2855, 1699, 1657, 1629, 1454, 1376, 1039 cm^{–1}; ECD (MeCN) λ_{max} ($\Delta\epsilon$) 209 (+3.70), 282 (+0.47), 326 (+0.11) nm; ¹H NMR (CD₃OD, 600 MHz) and ¹³C NMR (CD₃OD, 150 MHz) data, see Tables 1 and 2; (+)-HR-ESI-MS *m/z* 259.1666 [M+Na]⁺ (calcd for C₁₅H₂₄O₂Na, 259.1674). The original ¹H NMR, ¹³C NMR, DEPT, HSQC, ¹H-¹H COSY, HMBC, NOESY, IR, and (+)-HR-ESI-MS spectra are shown in Figures S6–S14, Supplementary Materials.

(+)-(1*R*,4*R*,9*S*,11*R*)-Caryophyll-8(13)-en-14-ol-5-one (2): colorless oil; $[\alpha]_{\text{D}}^{20}$ + 7.14 (*c* 0.03, MeOH); IR ν_{max} 3444, 3420, 2957, 2928, 2855, 1699, 1629, 1451, 1378, 1083, 1034, 888 cm^{–1}; ECD (MeCN) λ_{max} ($\Delta\epsilon$) 207 (+7.25), 295 (+1.62); ¹H NMR (CD₃OD, 600 MHz) and ¹³C NMR (CD₃OD, 150 MHz) data, see Tables 1 and 2; (+)-HR-ESI-MS *m/z* 259.1666 [M+Na]⁺ (calcd for C₁₅H₂₄O₂Na, 259.1674). The original ¹H NMR, ¹³C NMR, DEPT, HSQC, ¹H-¹H COSY, HMBC, NOESY, 1D NOE, IR, and (+)-HR-ESI-MS spectra are shown in Figures S15–S24, Supplementary Materials.

(–)-(3*Z*,1*R*,5*S*,8*S*,9*S*,11*R*)-5,8-Epoxycaryophyll-3-en-14-*O*-β-D-glucopyranoside (3): colorless oil; $[\alpha]_{\text{D}}^{20}$ – 15.0 (*c* 0.02, MeOH); IR ν_{max} 3400, 2964, 2923, 2865, 1637, 1454, 1417, 1381, 1078, 1039 cm^{–1}; ¹H NMR (CD₃OD, 600 MHz) and ¹³C NMR (CD₃OD, 150 MHz) data, see Tables 1 and 2; (+)-HR-ESI-MS *m/z* 421.2196 [M+Na]⁺ (calcd for C₂₁H₃₄O₇Na, 421.2202). The original ¹H NMR, ¹³C NMR, DEPT, HSQC, ¹H-¹H COSY, HMBC, NOESY, 1D NOE, IR, and (+)-HR-ESI-MS spectra are shown in Figures S25–S34, Supplementary Materials.

(–)-(3*Z*,1*R*,5*S*,8*S*,9*S*,11*R*)-5,8-Epoxycaryophyll-3-en-14-ol (3a): colorless oil; $[\alpha]_{\text{D}}^{20}$ – 4.8 (*c* 0.04, MeOH); ECD (MeCN) λ_{max} ($\Delta\epsilon$) 211 (+0.29), 251 (+0.05) nm; ¹H NMR (CD₃OD, 600 MHz) data, see Table 1. (+)-HR-ESI-MS *m/z* 259.1667 [M+Na]⁺ (calcd for C₁₅H₂₄O₂Na, 259.1674). The original ¹H NMR and (+)-HR-ESI-MS spectra are shown in Figures S35 and S36, Supplementary Materials.

(+)-(1*S*,7*R*,10*S*)-Guai-4-en-3-one-11-*O*-β-D-fucopyranoside (4): colorless oil; $[\alpha]_{\text{D}}^{20}$ + 29.4 (*c* 0.02, MeOH); IR ν_{max} 3403, 2923, 2852, 1676, 1623, 1464, 1386, 1172, 1065 cm^{–1}; ¹H NMR (CD₃OD, 600 MHz) and ¹³C NMR (CD₃OD, 150 MHz) data, see Tables 2 and 3; (+)-HR-ESI-MS at *m/z* 405.2244 [M+Na]⁺ (calcd for C₂₁H₃₄O₆Na, 405.2253). The original ¹H NMR, ¹³C NMR, DEPT, HSQC, ¹H-¹H COSY, HMBC, NOESY, IR, and (+)-HR-ESI-MS spectra are shown in Figures S37–S45, Supplementary Materials.

(+)-(1*S*,7*R*,10*S*)-Guai-4-en-11-ol-3-one (**4a**): colorless oil; $[\alpha]_D^{20} + 26.7$ (*c* 0.03, MeOH); ECD (MeCN) λ_{\max} ($\Delta\epsilon$) 234 (+1.54), 318 (−0.19), 324 (−0.20) nm; ^1H NMR (CD_3OD , 600 MHz) data, see Table 3. (+)-HR-ESI-MS at m/z 259.1673 $[\text{M}+\text{Na}]^+$, (calcd for $\text{C}_{15}\text{H}_{24}\text{O}_2\text{Na}$, 259.1668). The original ^1H NMR and (+)-HR-ESI-MS spectra are shown in Figures S46 and S47, Supplementary Materials.

(−)-(2*R*,5*R*,10*R*)-Vetispir-6-en-8-one-11-*O*- β -D-fucopyranoside (**5**): colorless oil; $[\alpha]_D^{20} - 28.2$ (*c* 0.04, MeOH); IR ν_{\max} 3303, 2972, 2925, 1665, 1467, 1381, 1170, 1070, 990 cm^{-1} ; ^1H NMR (CD_3OD , 600 MHz) and ^{13}C NMR (CD_3OD , 150 MHz) data, see Tables 2 and 3; (+)-HR-ESI-MS at m/z 405.2250 $[\text{M}+\text{Na}]^+$ (calcd for $\text{C}_{21}\text{H}_{34}\text{O}_6\text{Na}$ 405.2253). The original ^1H NMR, ^{13}C NMR, DEPT, HSQC, ^1H - ^1H COSY, HMBC, NOESY, IR, and (+)-HR-ESI-MS spectra are shown in Figures S48–S56, Supplementary Materials.

(−)-(2*R*,5*R*,10*R*)-Vetispir-6-en-11-ol-8-one (**5a**): colorless oil; $[\alpha]_D^{20} - 15.0$ (*c* 0.02, MeOH); ECD (MeCN) λ_{\max} ($\Delta\epsilon$) 235 (−1.74) nm; ^1H NMR (CD_3OD , 600 MHz) data, see Table 3. (+)-HR-ESI-MS at m/z 259.1673 $[\text{M}+\text{Na}]^+$ (calcd for $\text{C}_{15}\text{H}_{24}\text{O}_2\text{Na}$, 259.1674). The original ^1H NMR and (+)-HR-ESI-MS spectra are shown in Figures S57 and S58, Supplementary Materials.

3.5. Enzymatic Hydrolysis of Compounds 3–5

Snailase (20 mg) was used to hydrolyze compound **3** in water (5.0 mL) for 48 h at 37 °C. The aglycone (compound **3a**, 0.8 mg) was extracted by EtOAc (4 × 5 mL) in a liquid–liquid extractor and purified by HPLC. Compounds **4** (2 mg) and **5** (1.2 mg) were enzymatically hydrolyzed as above to obtain compounds **4a** (0.8 mg) and **5a** (0.5 mg).

3.6. ECD Calculation

The details of ECD calculation of compounds **1**, **2**, and **3a–5a** are shown in Texts S2–S6, Figures S1–S5, and Tables S1–S5 Supplementary Materials).

3.7. Cell Viability Assay

RAW264.7 cells were grown in DMEM supplemented with 10% FBS under a humidified environment at 37 °C and 5% CO_2 . The cells were planted in 96-well plates (3×10^4 cells/well) and incubated with compounds **1–5** and **3a–5a** (25, 50, and 100 μM) for one day. Then, the cells were treated by CCK-8 solution (10 μL /well) and incubated for 1 h. Under 450 nm, the absorbance of each well was tested to evaluate the viability of the cells.

3.8. Nile Red Staining

RAW264.7 cells were placed in 96-well plates (3×10^4 cells/well). Then, the cells were treated with ox-LDL (75 $\mu\text{g}/\text{mL}$), together with compounds **1–5** and **3a–5a** (25, 50, and 100 μM). After incubation for 24 h, the cells were kept for 30 min at 37 °C with 4% paraformaldehyde, then rinsed with PBS. The cells were hatched with freshly prepared Nile Red staining solution (2 $\mu\text{g}/\text{mL}$) for 30 min. Finally, PBS was used to wash the cells, and the fluorescence intensity was measured at 530 nm/590 nm.

3.9. Oil Red O Staining

RAW264.7 cells were placed in 24-well plates (3×10^5 cells/well). Then, the cells were treated with ox-LDL (75 $\mu\text{g}/\text{mL}$) and compound **4** (25, 50, and 100 μM). After incubation for 24 h, the cells were kept for 30 min at 37 °C with 4% paraformaldehyde, followed by rinsing with PBS. The cells were washed with 50% isopropanol for 20 s, and incubated with fresh-filtered Oil Red O solution (60% saturated Oil Red O/40% deionized water) for 30 min. The cells were washed with alternate rinses of 50% isopropanol and PBS to remove the floating colors and photographed for observation by fluorescence microscopy. Finally, the cells were washed with isopropanol, and the absorbance was observed at 550 nm.

3.10. ELISA

RAW264.7 cells (1×10^6 /well) were placed into six-well culture plates and treated by the above method. The contents of TC and FC were measured using the ELISA kits.

4. Conclusions

In conclusion, five new sesquiterpenoids were isolated from safflower, including caryophyllane-type, guaiane-type, and vetispirane-type sesquiterpenoids. The sesquiterpenoid types characterized herein have not been reported from *C. tinctorius*, and compounds **4** and **5** are rare sesquiterpenoid fucopyranosides. The sesquiterpenoids showed significant anti-atherosclerosis activity by decreasing the contents of lipid, TC, and FC in ox-LDL-treated RAW264.7 cells. Altogether, these new sesquiterpenoids not only enrich the diversity of sesquiterpenoids in safflower but also explain the effective material basis of safflower in treating AS.

Supplementary Materials: The following are available online at <https://www.mdpi.com/article/10.3390/nu14245348/s1>, Figure S1: ω B97XD/DGDZVP optimized 21 conformers of (1*R*,4*S*,9*S*,11*R*)-**1**, Figure S2: ω B97XD/DGDZVP optimized 18 conformers of (1*R*,4*R*,9*S*,11*R*)-**2**, Figure S3: ω B97XD/DGDZVP optimized 9 conformers of (1*R*,5*S*,8*S*,9*S*,11*R*)-**3a**, Figure S4: ω B97XD/DGDZVP optimized 8 conformers of (1*S*,7*R*,10*S*)-**4a**, Figure S5: ω B97XD/DGDZVP optimized 15 conformers of (2*R*,5*R*,10*R*)-**5a**, Figure S6: The ^1H NMR spectrum of compound **1** in CD_3OD , Figure S7: The ^{13}C NMR spectrum of compound **1** in CD_3OD , Figure S8: The DEPT spectrum of compound **1** in CD_3OD , Figure S9: The HSQC spectrum of compound **1** in CD_3OD , Figure S10: The ^1H - ^1H COSY spectrum of compound **1** in CD_3OD , Figure S11: The HMBC spectrum of compound **1** in CD_3OD , Figure S12: The NOESY spectrum of compound **1** in CD_3OD , Figure S13: The IR spectrum of compound **1**, Figure S14: The (+)-HR-ESI-MS spectroscopic data of compound **1**, Figure S15: The ^1H NMR spectrum of compound **2** in CD_3OD , Figure S16: The ^{13}C NMR spectrum of compound **2** in CD_3OD , Figure S17: The DEPT spectrum of compound **2** in CD_3OD , Figure S18: The HSQC spectrum of compound **2** in CD_3OD , Figure S19: The ^1H - ^1H COSY spectrum of compound **2** in CD_3OD , Figure S20: The HMBC spectrum of compound **2** in CD_3OD , Figure S21: The NOESY spectrum of compound **2** in CD_3OD , Figure S22: The 1D NOE spectrum of compound **2** in CD_3OD , Figure S23: The IR spectrum of compound **2**, Figure S24: The (+)-HR-ESI-MS spectroscopic data of compound **2**, Figure S25: The ^1H NMR spectrum of compound **3** in CD_3OD , Figure S26: The ^{13}C NMR spectrum of compound **3** in CD_3OD , Figure S27: The DEPT spectrum of compound **3** in CD_3OD , Figure S28: The HSQC spectrum of compound **3** in CD_3OD , Figure S29: The ^1H - ^1H COSY spectrum of compound **3** in CD_3OD , Figure S30: The HMBC spectrum of compound **3** in CD_3OD , Figure S31: The NOESY spectrum of compound **3** in CD_3OD , Figure S32: The 1D NOE spectrum of compound **3** in CD_3OD , Figure S33: The IR spectrum of compound **3**, Figure S34: The (+)-HR-ESI-MS spectroscopic data of compound **3**, Figure S35: The ^1H NMR spectrum of compound **3a** in CD_3OD , Figure S36: The (+)-HR-ESI-MS spectroscopic data of compound **3a**, Figure S37: The ^1H NMR spectrum of compound **4** in CD_3OD , Figure S38: The ^{13}C NMR spectrum of compound **4** in CD_3OD , Figure S39: The DEPT spectrum of compound **4** in CD_3OD , Figure S40: The HSQC spectrum of compound **4** in CD_3OD , Figure S41: The ^1H - ^1H COSY spectrum of compound **4** in CD_3OD , Figure S42: The HMBC spectrum of compound **4** in CD_3OD , Figure S43: The NOESY spectrum of compound **4** in CD_3OD , Figure S44: The IR spectrum of compound **4**, Figure S45: The (+)-HR-ESI-MS spectroscopic data of compound **4**, Figure S46: The ^1H NMR spectrum of compound **4a** in CD_3OD , Figure S47: The (+)-HR-ESI-MS spectroscopic data of compound **4a**, Figure S48: The ^1H NMR spectrum of compound **5** in CD_3OD , Figure S49: The ^{13}C NMR spectrum of compound **5** in CD_3OD , Figure S50: The DEPT spectrum of compound **5** in CD_3OD , Figure S51: The HSQC spectrum of compound **5** in CD_3OD , Figure S52: The ^1H - ^1H COSY spectrum of compound **5** in CD_3OD , Figure S53: The HMBC spectrum of compound **5** in CD_3OD , Figure S54: The NOESY spectrum of compound **5** in CD_3OD , Figure S55: The IR spectrum of compound **5**, Figure S56: The (+)-HR-ESI-MS spectroscopic data of compound **5**, Figure S57: The ^1H NMR spectrum of compound **5a** in CD_3OD , Figure S58: The (+)-HR-ESI-MS spectroscopic data of compound **5a**, Table S1: Energy analysis for the conformers of (1*R*,4*S*,9*S*,11*R*)-**1**, Table S2: Energy analysis for the conformers of (1*R*,4*R*,9*S*,11*R*)-**2**, Table S3: Energy analysis for the conformers of (1*R*,5*S*,8*S*,9*S*,11*R*)-**3a**, Table S4: Energy analysis for the conformers of (1*S*,7*R*,10*S*)-**4a**; Table S5: Energy analysis for the conformers of (2*R*,5*R*,10*R*)-**5a**, Text S1: General experimental details, Text S2: ECD calculation of compound **1**, Text S3: ECD calculation of compound **2**, Text S4: ECD calculation of compound **3a**, Text S5: ECD calculation of compound **4a**, Text S6: ECD calculation of compound **5a**, Supplementary References [32–36].

Author Contributions: Conceptualization, C.P. and L.X.; methodology, L.L., Y.G. and Y.F.; investigation, L.L., J.L., X.L. and H.S.; validation, J.L. and G.W.; writing—original draft, L.L.; writing—review and editing, L.X.; supervision, C.P. and L.X.; project administration, L.X.; funding acquisition, C.P. and L.X. All authors have read and agreed to the published version of the manuscript.

Funding: This research was funded by the National Natural Science Foundation of China (NNSFC; Grant Nos. 82022072 and U19A2010), the Fok Ying Tung Education Foundation (Grant No. 171037), the “Xinglin Scholar” Plan of Chengdu University of Traditional Chinese Medicine (Grant No. XKTD2022006), and the Innovation Team and Talents Cultivation Program of the National Administration of Traditional Chinese Medicine (Grant No. ZYYCXTD-D-202209).

Data Availability Statement: The data presented in this study are available in the Supplementary Materials or can be provided by the authors.

Conflicts of Interest: The authors declare no conflict of interest.

References

1. Cao, H.; Jia, Q.; Yan, L.; Chen, C.; Xing, S.; Shen, D. Quercetin suppresses the progression of atherosclerosis by regulating MST1-mediated autophagy in ox-LDL-induced RAW264.7 macrophage foam cells. *Int. J. Mol. Sci.* **2019**, *20*, 6093. [[CrossRef](#)] [[PubMed](#)]
2. Chen, F.; Guo, N.; Cao, G.; Zhou, J.; Yuan, Z. Molecular analysis of curcumin-induced polarization of murine RAW264.7 macrophages. *J. Cardiovasc. Pharmacol.* **2014**, *63*, 544–552. [[CrossRef](#)] [[PubMed](#)]
3. Wang, Y.; Jia, Q.; Zhang, Y.; Wei, J.; Liu, P. Taoren honghua drug attenuates atherosclerosis and plays an anti-inflammatory role in ApoE knock-out mice and RAW264.7 cells. *Front. Pharmacol.* **2020**, *11*, 1070. [[CrossRef](#)]
4. Yu, B.; Zhang, G.; Jin, L.; Zhang, B.; Yan, D.; Yang, H.; Ye, Z.; Ma, T. Inhibition of PAI-1 activity by toddalolactone as a mechanism for promoting blood circulation and removing stasis by Chinese herb *Zanthoxylum nitidum* var. *tomentosum*. *Front. Pharmacol.* **2017**, *8*, 489. [[CrossRef](#)]
5. Yuan, R.; Shi, W.L.; Xin, Q.Q.; Chen, K.J.; Cong, W.H. Holistic regulation of angiogenesis with chinese herbal medicines as a new option for coronary artery disease. *Evid.-Based Complement. Altern. Med.* **2018**, *2018*, 3725962. [[CrossRef](#)]
6. Bai, Y.; Lu, P.; Han, C.; Yu, C.; Chen, M.; He, F.; Yi, D.; Wu, L. Hydroxysafflower yellow A (HSYA) from flowers of *Carthamus tinctorius* L. and its vasodilatation effects on pulmonary artery. *Molecules* **2012**, *17*, 14918–14927. [[CrossRef](#)]
7. Wang, H.; Liu, J.; Yang, Y.; Cao, Q.; Huo, X.; Ma, S.; Hu, J.; Pavalko, F.M.; Liu, Q. Hydroxy-safflower yellow A inhibits the TNFR1-mediated classical NF- κ B pathway by inducing shedding of TNFR1. *Phytother. Res.* **2016**, *30*, 790–796. [[CrossRef](#)]
8. Yu, S.Y.; Lee, Y.J.; Kim, J.D.; Kang, S.N.; Lee, S.K.; Jang, J.Y.; Lee, H.K.; Lim, J.H.; Lee, O.H. Phenolic composition, antioxidant activity and anti-adipogenic effect of hot water extract from safflower (*Carthamus tinctorius* L.) seed. *Nutrients* **2013**, *5*, 4894–4907. [[CrossRef](#)]
9. Maneesai, P.; Prasarttong, P.; Bunbupha, S.; Kukongviriyapan, U.; Kukongviriyapan, V.; Tangsucharit, P.; Prachaney, P.; Pakdeechote, P. Synergistic antihypertensive effect of *Carthamus tinctorius* L. extract and captopril in L-NAME-induced hypertensive rats via restoration of eNOS and AT₁R expression. *Nutrients* **2016**, *8*, 122. [[CrossRef](#)]
10. Jeong, E.H.; Yang, H.; Kim, J.; Lee, K.W. Safflower seed oil and its active compound acacetin inhibit UVB-induced skin photoaging. *J. Microbiol. Biotechnol.* **2020**, *30*, 1567–1573. [[CrossRef](#)]
11. Ju, G.; Liu, Y. Study of safflower on blood lactate concentration and exercise function of mice after exercise. *Afr. J. Biotechnol.* **2011**, *10*, 9148–9152. [[CrossRef](#)]
12. Hong, H.; Lim, J.M.; Kothari, D.; Kwon, S.H.; Kwon, H.C.; Han, S.; Kim, S. Antioxidant properties and diet-related α -glucosidase and lipase inhibitory activities of yogurt supplemented with safflower (*Carthamus tinctorius* L.) petal extract. *Food Sci. Anim. Resour.* **2021**, *41*, 122–134. [[CrossRef](#)] [[PubMed](#)]
13. Mani, V.; Lee, S.; Yeo, Y.; Hahn, B. A metabolic perspective and opportunities in pharmacologically important safflower. *Metabolites* **2020**, *10*, 253. [[CrossRef](#)] [[PubMed](#)]
14. Tso, P.; Caldwell, J.; Lee, D.; Boivin, G.P.; DeMichele, S.J. Comparison of growth, serum biochemistries and n-6 fatty acid metabolism in rats fed diets supplemented with high-gamma-linolenic acid safflower oil or borage oil for 90 days. *Food Chem. Toxicol.* **2012**, *50*, 1911–1919. [[CrossRef](#)]
15. Yue, S.J.; Qu, C.; Zhang, P.X.; Tang, Y.P.; Jin, Y.; Jiang, J.S.; Yang, Y.N.; Zhang, P.C.; Duan, J.A. Carthorquinosides A and B, quinochalcone C-glycosides with diverse dimeric skeletons from *Carthamus tinctorius*. *J. Nat. Prod.* **2016**, *79*, 2644–2651. [[CrossRef](#)]
16. Zhang, H.; Duan, C.P.; Luo, X.; Feng, Z.M.; Yang, Y.N.; Zhang, X.; Jiang, J.S.; Zhang, P.C. Two new quinochalcone glycosides from the safflower yellow pigments. *J. Asian Nat. Prod. Res.* **2020**, *22*, 1130–1137. [[CrossRef](#)]
17. Yue, S.; Tang, Y.; Xu, C.; Li, S.; Zhu, Y.; Duan, J.A. Two new quinochalcone C-glycosides from the florets of *Carthamus tinctorius*. *Int. J. Mol. Sci.* **2014**, *15*, 16760–16771. [[CrossRef](#)]
18. Zhou, X.; Tang, L.; Xu, Y.; Zhou, G.; Wang, Z. Towards a better understanding of medicinal uses of *Carthamus tinctorius* L. in traditional Chinese medicine: A phytochemical and pharmacological review. *J. Ethnopharmacol.* **2014**, *151*, 27–43. [[CrossRef](#)]

19. Cazarolli, L.H.; Kappel, V.D.; Pereira, D.F.; Moresco, H.H.; Brighente, I.M.; Pizzolatti, M.G.; Silva, F.R. Anti-hyperglycemic action of apigenin-6-C- β -fucopyranoside from *Averrhoa carambola*. *Fitoterapia* **2012**, *83*, 1176–1183. [[CrossRef](#)]
20. Suzuki, R.; Okada, Y.; Okuyama, T. A new flavone C-glycoside from the style of *Zea mays* L. with glycation inhibitory activity. *Chem. Pharm. Bull.* **2003**, *51*, 1186–1188. [[CrossRef](#)]
21. Barrero, A.F.; Haïdour, A.; Sedqui, A.; Mansour, A.I.; Rodríguez-García, I.; López, A.; Muñoz-Dorado, M. Saikosaponins from roots of *Bupleurum gibraltarium* and *Bupleurum spinosum*. *Phytochemistry* **2000**, *54*, 741–745. [[CrossRef](#)] [[PubMed](#)]
22. Liu, Z.; Jia, Z.; Cates, R.G.; Li, D.; Owen, N.L. Triterpenoid saponins from *Clinopodium chinensis*. *J. Nat. Prod.* **1995**, *58*, 184–188. [[CrossRef](#)] [[PubMed](#)]
23. Eskander, J.; Lavaud, C.; Harakat, D. Steroidal saponins from the leaves of *Beaucarnea recurvata*. *Phytochemistry* **2011**, *72*, 946–951. [[CrossRef](#)] [[PubMed](#)]
24. Chen, S.P.; Su, J.H.; Yeh, H.C.; Ahmed, A.F.; Dai, C.F.; Wu, Y.C.; Sheu, J.H. Novel norhumulene and xeniaphyllane-derived terpenoids from a formosan soft coral *Sinularia gibberosa*. *Chem. Pharm. Bull.* **2009**, *57*, 162–166. [[CrossRef](#)]
25. Li, X.R.; Liu, J.; Peng, C.; Zhou, Q.M.; Liu, F.; Guo, L.; Xiong, L. Polyacetylene glucosides from the florets of *Carthamus tinctorius* and their anti-inflammatory activity. *Phytochemistry* **2021**, *187*, 112770. [[CrossRef](#)]
26. Tsui, W.Y.; Brown, G. Acid-catalysed rearrangement of caryophyllene oxide. *J. Chem. Soc. Perkin Trans.* **1996**, *1*, 2507–2509. [[CrossRef](#)]
27. Yu, Y.; Gao, H.; Dai, Y.; Xiao, G.K.; Zhu, H.J.; Yao, X.S. Guaiane-type sesquiterpenoid glucosides from *Gardenia jasminoides* Ellis. *Magn. Reson. Chem.* **2011**, *49*, 258–261. [[CrossRef](#)]
28. Tagliatalata-Scafati, O.; Pollastro, F.; Cicione, L.; Chianese, G.; Bellido, M.L.; Munoz, E.; Ozen, H.C.; Toker, Z.; Appendino, G. STAT-3 inhibitory bisabolanes from *Carthamus glaucus*. *J. Nat. Prod.* **2012**, *75*, 453–458. [[CrossRef](#)]
29. Yin, X.; Liu, Y.; Pan, J.; Ye, H.L.; Sun, Y.; Zhao, D.Y.; Kuang, H.X.; Yang, B.Y. Melongenaterpenes A-L, vetispirane-type sesquiterpenoids from the roots of *Solanum melongena*. *J. Nat. Prod.* **2019**, *82*, 3242–3248. [[CrossRef](#)]
30. Liu, B.; Zhang, B.; Guo, R.; Li, S.; Xu, Y. Enhancement in efferocytosis of oxidized low-density lipoprotein-induced apoptotic RAW264.7 cells through Sirt1-mediated autophagy. *Int. J. Mol. Med.* **2014**, *33*, 523–533. [[CrossRef](#)]
31. Yuan, Y.; Li, P.; Ye, J. Lipid homeostasis and the formation of macrophage-derived foam cells in atherosclerosis. *Protein Cell* **2012**, *3*, 173–181. [[CrossRef](#)] [[PubMed](#)]
32. Gotō, H.; Ōsawa, E. Corner flapping: A simple and fast algorithm for exhaustive generation of ring conformations. *J. Am. Chem. Soc.* **1989**, *111*, 8950–8951. [[CrossRef](#)]
33. Gotō, H.; Ōsawa, E. An efficient algorithm for searching low-energy conformers of cyclic and acyclic molecules. *J. Chem. Soc. Perkin Trans.* **1993**, *2*, 187–198. [[CrossRef](#)]
34. *Gaussian 16*, Revision B.01; Gaussian, Inc.: Wallingford, CT, USA, 2006.
35. Liu, Y.; Liu, F.; Qiao, M.M.; Guo, L.; Chen, M.H.; Peng, C.; Xiong, L. Curcumanes A and B, two bicyclic sesquiterpenoids with significant vasorelaxant activity from *Curcuma longa*. *Org. Lett.* **2019**, *21*, 1197–1201. [[CrossRef](#)]
36. *Spec Dis*, Version 1.71; University of Würzburg: Würzburg, Germany, 2017.